

Supplemental Materials for manuscript:

Neumann et al. Involvement of fast-spiking cells in ictal sequences during spontaneous seizures in rats with chronic temporal lobe epilepsy. *Brain*, 2017.

Supplemental Figures

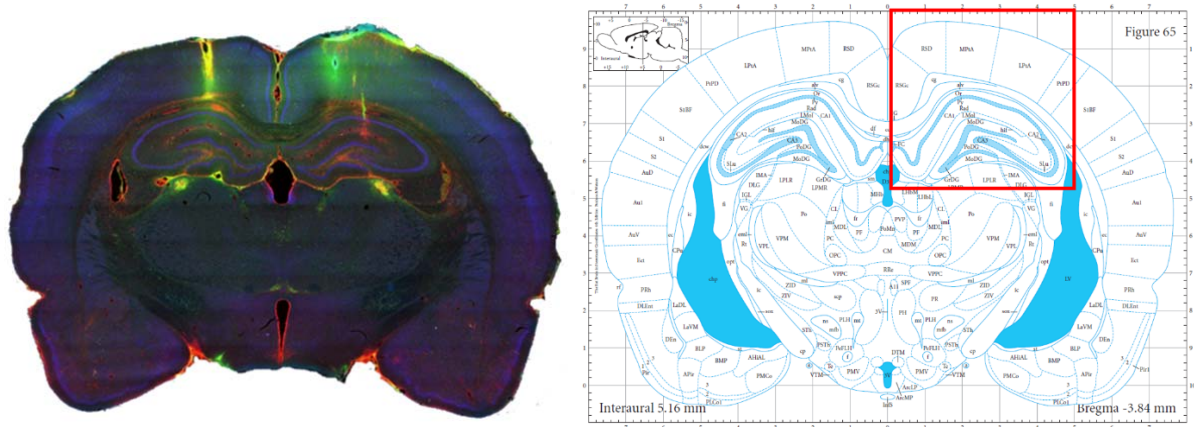


Figure S1. (left) Histological analysis for neurons (NeuN; blue), reactive astrocytes (Vimentin; red) and reactive microglia (Ox-42; anti-CD11b/c antibody; green) to verify electrode position. Traces in the right hemisphere correspond to tetrode locations and the trace in the left hemisphere corresponds to EEG electrode used for seizure monitoring before hyperdrive implantation. Note that although it is conceivable that damage induced by the electrode implants may induce seizures, based on substantial experience with these methods, we consider such a scenario to be unlikely. In fact, we noticed in several animals that the seizure rate was actually reduced after hyperdrive implantation, suggesting a lack of pro-epileptic effects of hyperdrive implantation in our experiments. (Right) Corresponding areas in brain atlas (Paxinos and Watson, 1986).

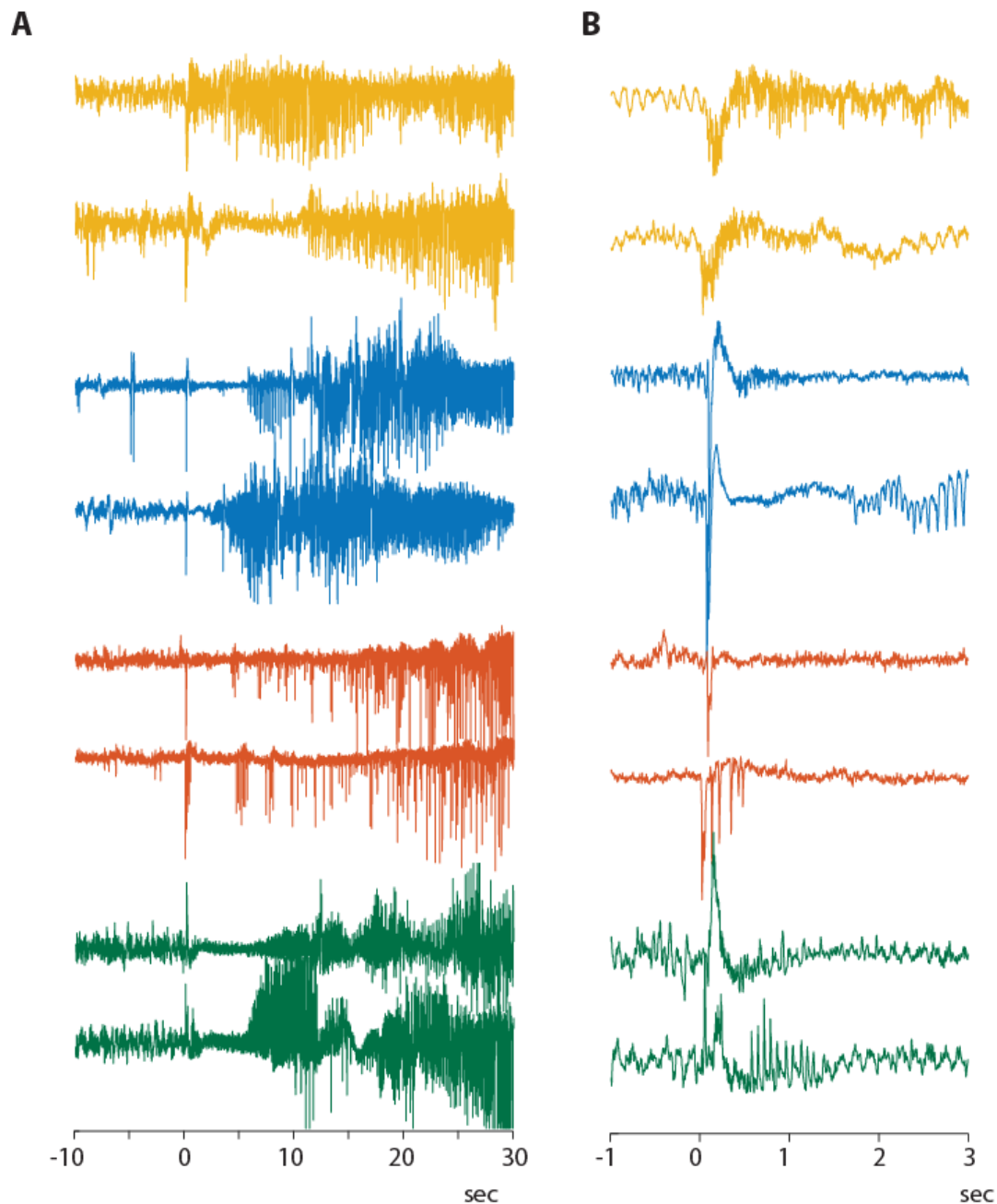


Figure S2 (A) Representative hippocampal LFP traces around seizure onset. Each trace is from a different seizure and the various colors represent different animals (green: KA animal). Although it is not always easy to clearly identify seizure type, the vast majority of the recorded seizures could be considered to be the low-voltage, fast activity type. (B) Traces at a faster time scale from the seizure onset periods from the corresponding traces in panel A.

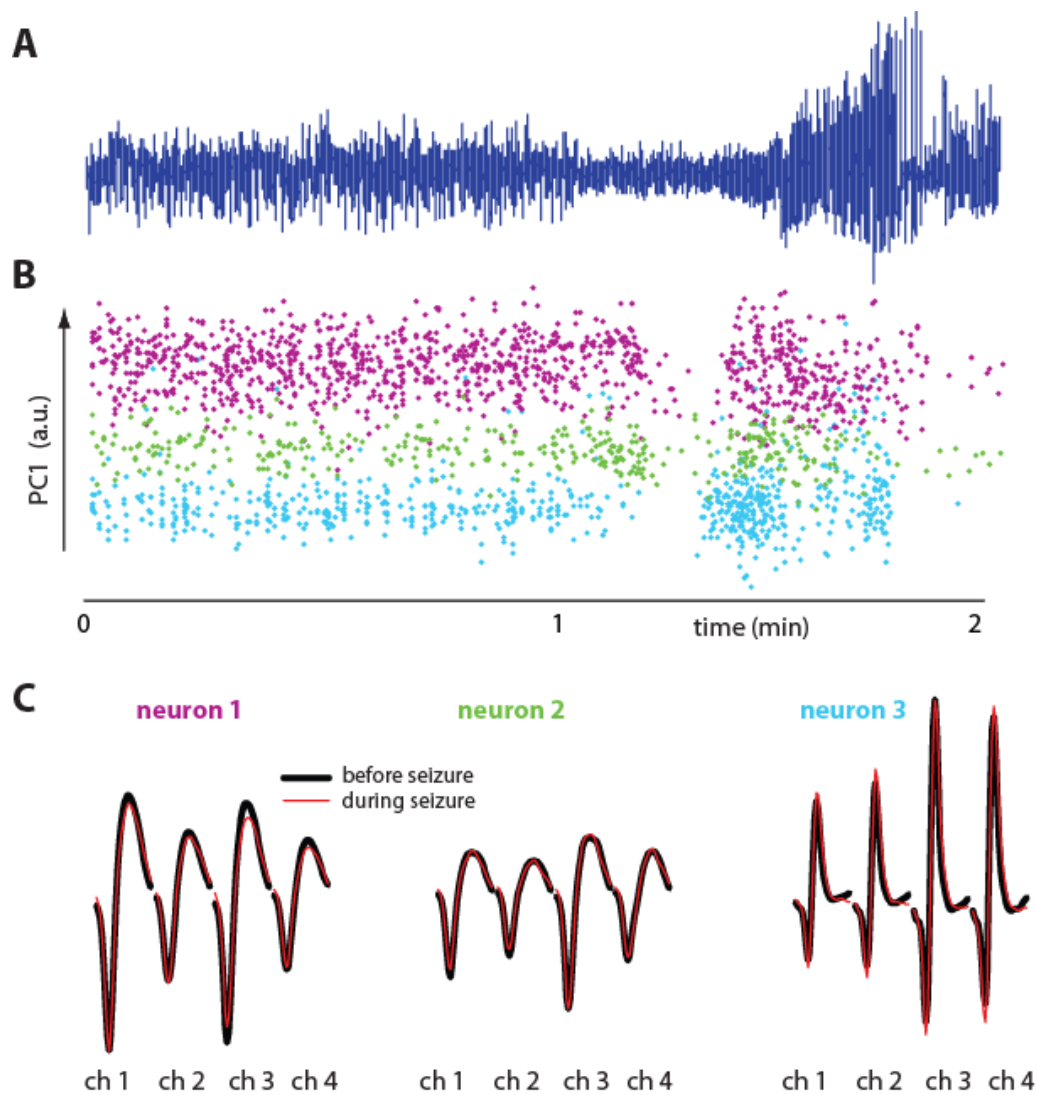


Figure S3. Consistency of spike waveforms before and during seizure. (A) Two minutes of sample hippocampal LFP around time of seizure. (B) Spikes in Principal Component (PC) space of three neurons recorded simultaneously on the same tetrode during seizure shown above. Each dot represents a single spike, and different colors correspond to spikes from different neurons. Distribution of points at consistent heights for each neuron shows that the spikes had consistent waveforms both before and during the seizure. (C) Average spike waveforms for the above neurons (color labels correspond to colors in B). Neurons 1 and 2 are putative pyramidal cells and neuron 3 is a putative interneuron. Superimposed black and red traces show average waveforms before and during seizure, respectively (see Methods for more details on spike sorting).

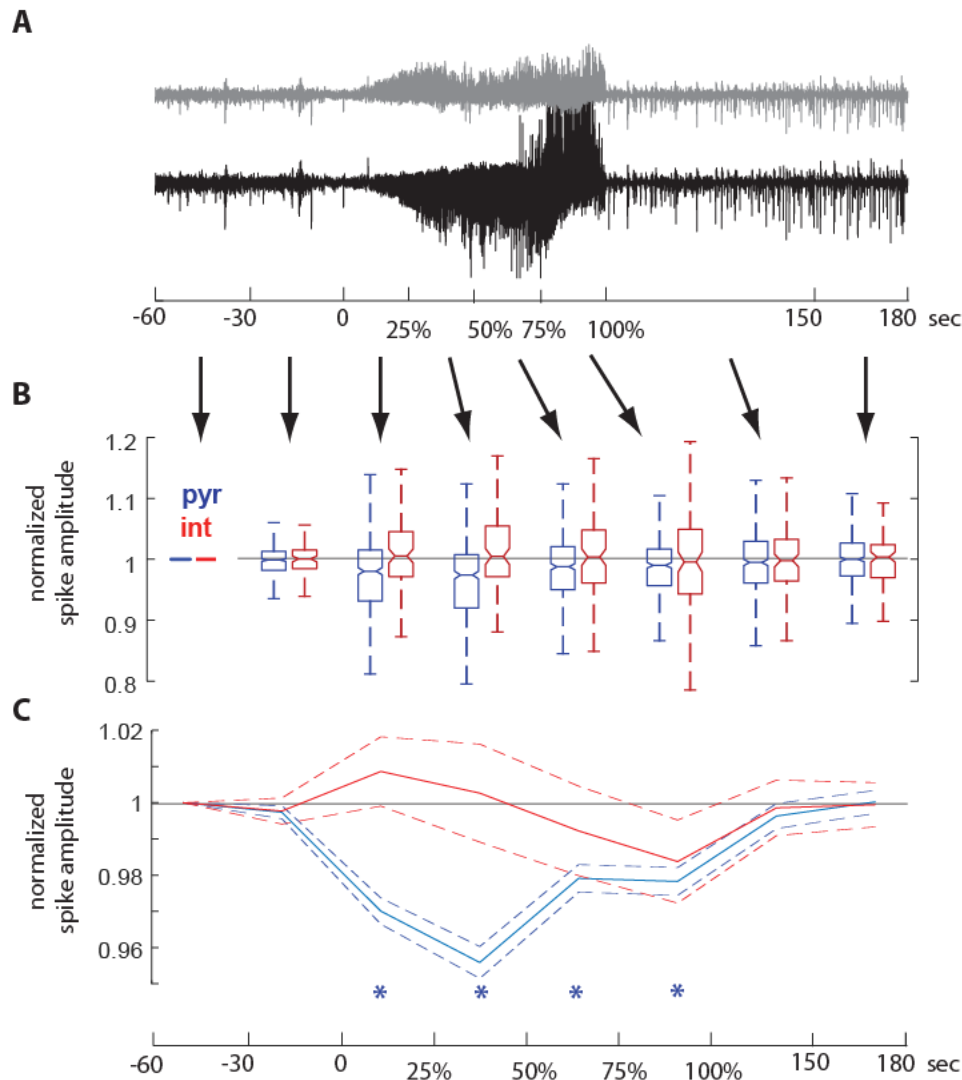


Figure S4. Assessment of the potential changes in neuronal spike amplitude during seizures. (A) Examples of two LFP channels recorded simultaneously during a seizure. For spike amplitude analyses we divided seizures in 4 equal parts corresponding to 25%, 50%, 75% and 100% of seizure duration. We also analysed spike amplitude in the periods between -60, -30 and 0 sec before seizure, and in the post-ictal transition period defined as from the end of the seizure till 150 sec, and in the period between 150 - 180sec after seizure. (B) Normalized spike amplitudes for all recorded neurons across different periods (blue: putative pyramidal cells; red: putative interneurons). For each neuron, spike amplitude was normalized by dividing it by the average spike amplitude for that neuron in period -60 -30 sec before seizure. For each box, the central mark indicates the median, and the bottom and top edges of the box indicate the 25th and 75th percentiles, respectively. The whiskers extend to the most extreme data points. (C) Summary statistics showing mean (solid line) \pm SEM (dashed lines) for data shown in (B). During all periods of seizure, amplitude of putative pyramidal cells was mildly but significantly reduced ($p < 0.0001$ denoted by stars; t-test). In contrast, for putative interneurons, we did not observe significant amplitude changes. Repeating the latter analyses separately for hippocampal and cortical neurons also showed significant amplitude reductions to be present only for the putative pyramidal cells.

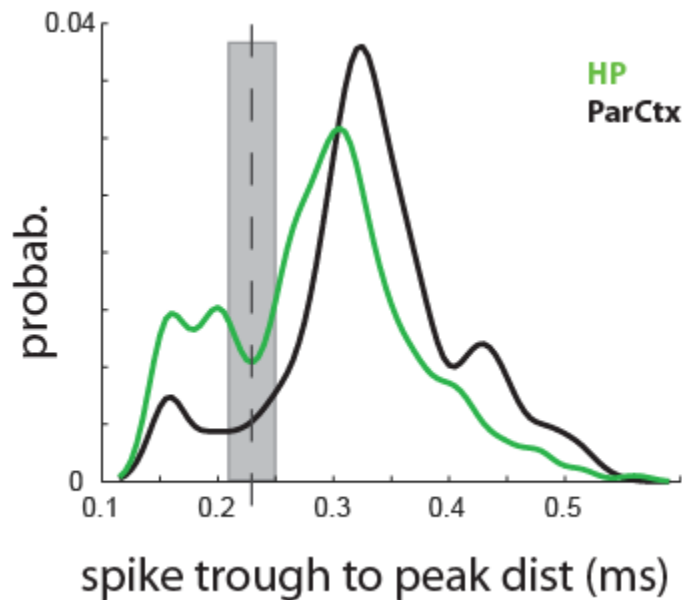


Figure S5. Probability distribution of spike trough-to-peak distances for hippocampal neurons (green) and neocortical neurons (black) (see Figure 3A). For these analyses, we used trough-to-peak distances of 0.23ms as a border between putative interneurons and pyramidal cells (dashed line). Changing trough-to-peak distance criteria by ± 0.02 ms (gray area) did not affect qualitative results for any of the subsequent analyses. For verification of the spike shape-based classification, we also used functional characteristics such as the shape of the cross-correlograms, auto-correlograms, and firing rates (see Methods), which showed strong agreement and consistency with 0.23 ms threshold. In addition, to avoid relying on specific threshold values for discriminating putative interneurons and pyramidal cells, we repeated the main analyses shown in Figure 3B&C by measuring correlation coefficients between trough-to-peak distances and LFP entrainment (see Results), which further validated our conclusions.

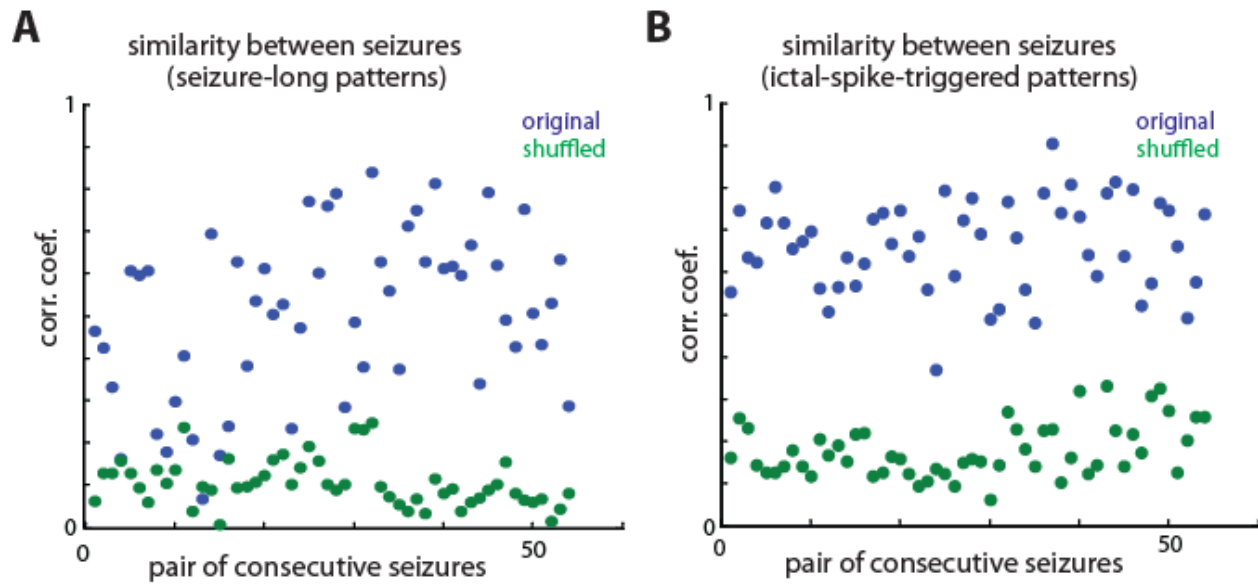


Figure S6. (A) Similarity between seizure-long patterns for consecutive pairs of seizures in a single 24 h recording period which had 55 seizures. Each point represents similarity between 2 consecutive seizures (see Figure 1C for sample patterns; original data - blue; neuron shuffled data - green). To quantify similarity, activity of each neuron was smoothed with 10 sec Gaussian kernel and normalized to zero mean and unit SD (see Figure 1C), and for each neuron, a correlation coefficient was calculated between its activity in two consecutive seizures, and averaged across all active neurons. (B) Similarity of ictal-spike-triggered patterns between consecutive pairs of seizures for the same data set as in panel A (see Fig. 1G for sample patterns). For each neuron, its ictal-spike-triggered activity was calculated (Figure 1G), and the correlation coefficient was taken between its triggered activity in two consecutive seizures, and averaged across all strongly entertained neurons. Correlation values for original data are marked in blue and neuron shuffled data in green.

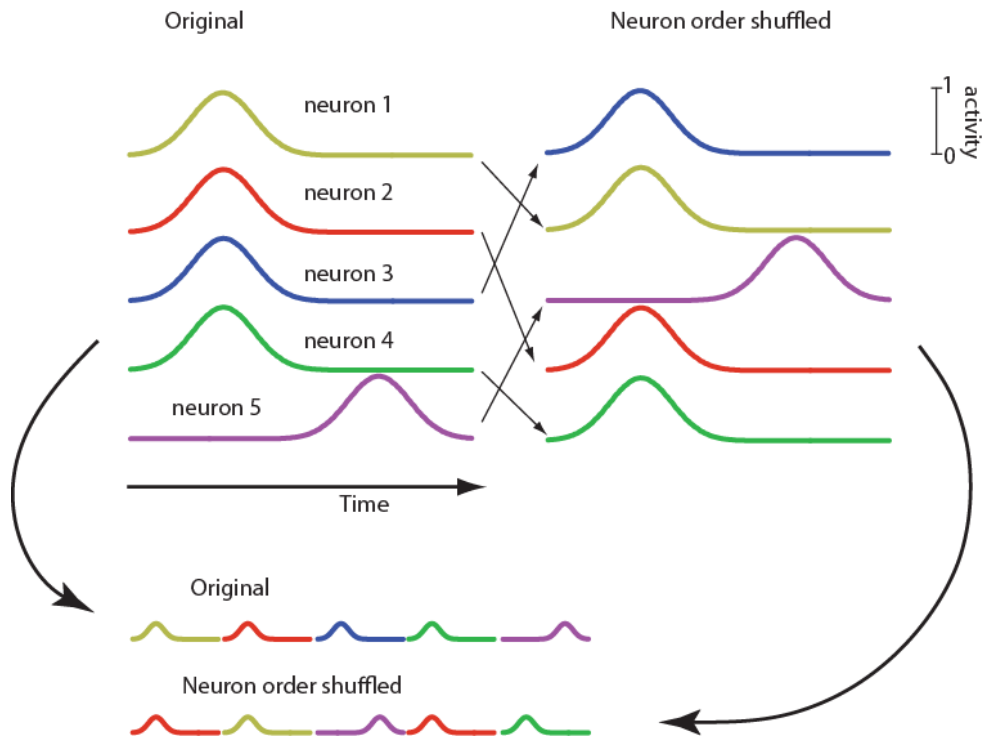


Figure S7. Cartoon illustration of shuffling neuronal order. (Top left) Activity of 5 neurons where neurons 1-4 are active at the same time. (Top right) Activity of the same neurons after shuffling its order. (Bottom) Activity of all neurons shown as a single vector for original and shuffled data respectively. Note that despite shuffling, the correlation coefficient between both vectors will be positive, as majority of neurons have similar activity profile. Therefore this shuffling procedure results here in a more difficult to reject null hypothesis as compared to spike time shuffling procedures. To verify if this was also true for our data, we repeated all analyses using spike time shuffling with preserved inter-spike-interval distributions. As expected, due to the similarity of activity patterns between neurons, those analyses gave even more significant p values as compared to neuronal order shuffling approach.

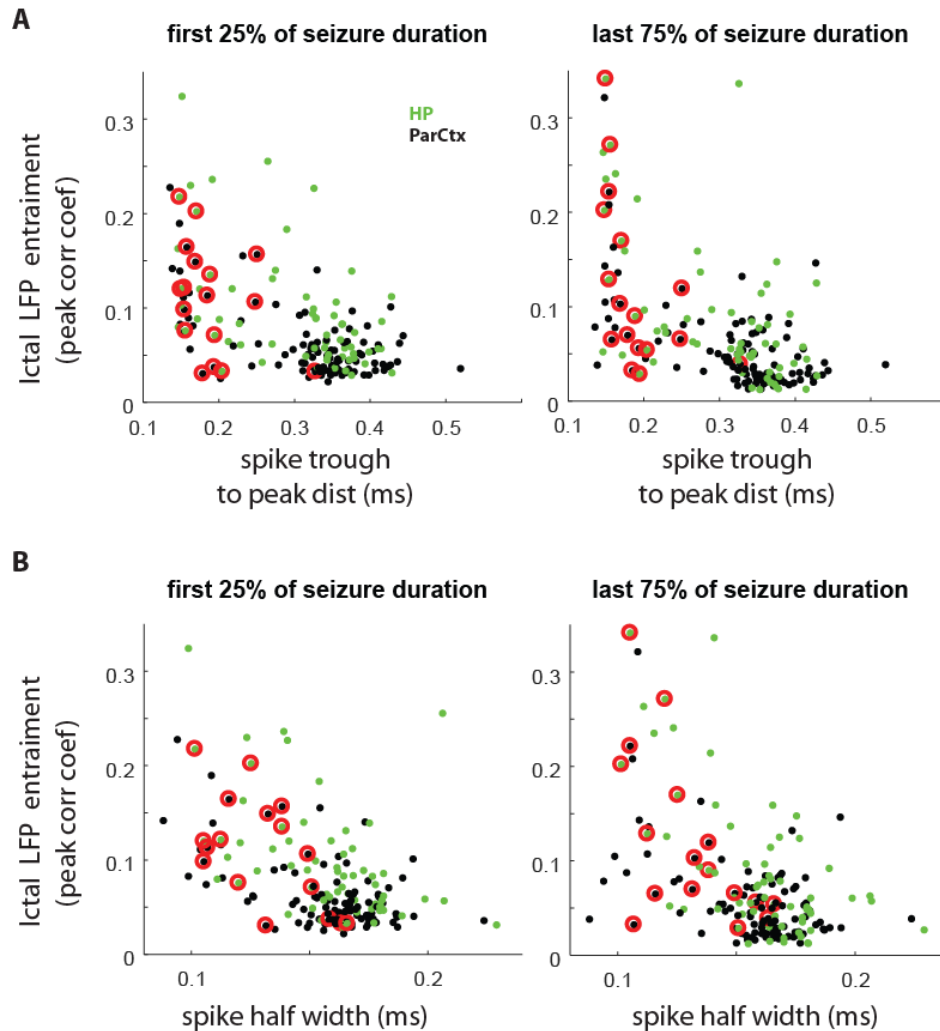


Figure S8. (A) Relationship between the entrainment to ictal spikes and the neuronal spike width calculated separately during the first 25% of seizure duration (left), and the last 75% of seizure duration (right). Consistent with the results shown in Fig. 3C, we found significant negative correlation between entrainment to ictal LFP and half-width of spikes for both early and late parts of seizure (first 25%: HP: $r = -0.5$, $p < 0.001$; ParCtx: $r = -0.59$, $p < 0.001$; last 75%: HP: $r = -0.56$, $p < 0.001$; ParCtx: $r = -0.58$, $p < 0.001$). (B) Relationship between entrainment to ictal spikes and spike trough-to-peak distance during the first 25% (left), and the last 75% of seizure duration (first 25% HP: $r = -0.51$, $p < 0.001$; ParCtx: $r = -0.56$, $p < 0.001$; last 75%: HP: $r = -0.67$, $p < 0.001$; ParCtx: $r = -0.49$, $p < 0.001$). Plot convention is the same as in Fig 3 B,C.

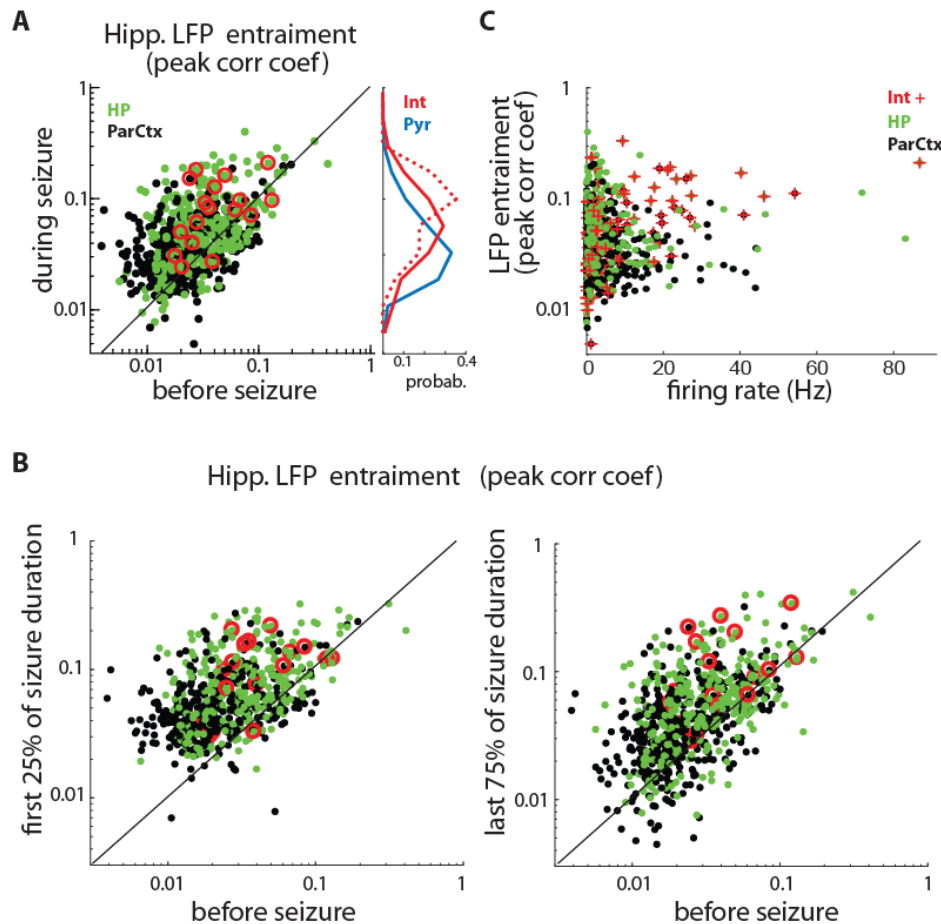


Figure S9. (A) Relationship between neuronal entrainment to hippocampal LFP before and during seizures, with the insert showing distribution of putative pyramidal cells (blue) and putative interneurons (red). Distribution of entrainment values was significantly different for putative interneurons and pyramidal cells ($p < 0.001$, Kolmogorov–Smirnov test). Dashed line shows distribution of putative interneurons which in addition to narrow spikes also displayed in conjuncture three other typical features of interneurons (firing rate above 15Hz, short latency inhibition to other cell, and most often inter-spike interval between 7ms–40ms); those cells are marked with red circles. (B) Relation between entrainment to hippocampal LFP before and during seizure for different periods of seizures (left: the first 25% of seizure duration; right: the last 75% of seizure duration). Consistent with results shown in Fig. 4, correlation between entrainment to ictal LFP was significant for both early and late parts of seizure (first 25%: HP: $r = 0.42$, $p < 0.001$; ParCtx: $r = 0.43$, $p < 0.001$; last 75%: HP: $r = 0.51$, $p < 0.001$; ParCtx: $r = 0.54$, $p < 0.001$). (C) Relation between LFP entrainment and peak firing rate. Green dots represent hippocampal neurons, and black dots correspond to neocortical neurons. Red crosses on top of dots indicate putative interneuron. For putative pyramidal cells we found no significant correlation between firing rate and LFP entrainment (HP $r = -0.07$, $p = 0.27$; ParCtx: $r = -0.07$, $p = 0.34$), however for putative interneurons we found significant positive correlation (HP: $r = 0.49$, $p < 0.0001$; ParCtx: $r = 0.52$, $p < 0.0001$). One possible explanation could be that a group of putative interneurons could contain multiple types of cells with narrow spikes, but only the subgroup characterized by high firing rate has strong LFP entrainment.

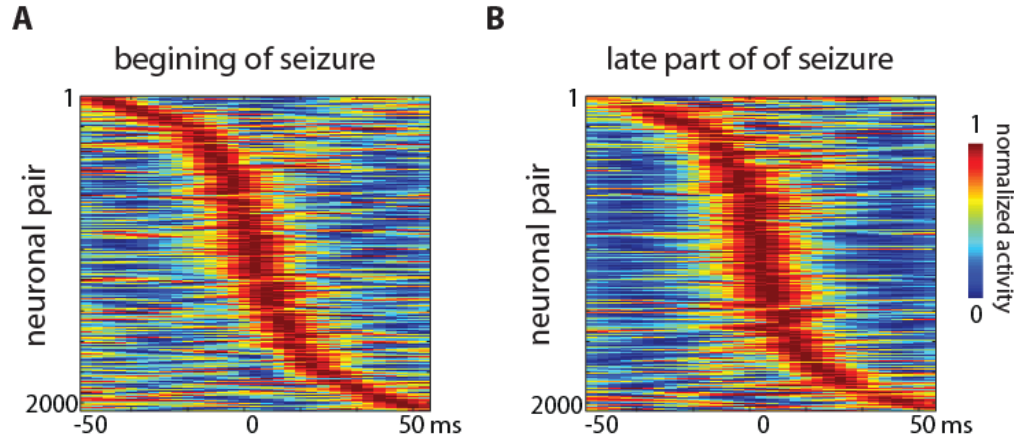


Figure S10. Sample cross-correlograms between pairs of neurons calculated during the beginning (A) and the later portion of the seizure (B). Plot convention is the same as in Fig. 6. For both periods (first 25% and last 75% of seizure duration), the structure of the cross-correlograms was similar to the cross-correlograms from the pre-seizure period ($r_{25\%}=0.31 \pm 0.057$, $r_{25\%shuffl}=0.16 \pm 0.048$, $p=0.0016$; $r_{75\%}=0.29 \pm 0.052$, $r_{75\%shuffl}=0.16 \pm 0.042$, $p=0.0085$; paired t-test).

Additional analyses.

In Suppl. Figures S8-10, we showed that our results are consistent across different phases of seizures. In addition, we repeated the same main analyses separately for seizures preceded by high or low theta activity, for seizures preceded by interictal spikes or without interictal spikes, and for seizures terminating with or without post-ictal suppression. In all cases, we found qualitatively consistent results with data presented in the main manuscript (data not shown). This suggests that preferential entrainment of putative interneurons to ictal activity, and the similarity of the relationships between neurons before and during seizure, are consistent properties of epileptic networks.

References

Paxinos G, Watson C. The rat in stereotaxic coordinates. San Diego, CA: Academic Press; 1986.